American Journal of Nanoscience and Nanotechnology
2014; 2(3): 45-49
Published online June 10, 2014 (http://www.sciencepublishinggroup.com/j/nano)
doi: 10.11648/j.nano.20140203.13

A theoretical study of the electronic properties of $Cd_{1-x}Zn_xS$ quantum dot superlattices

Saber Marzougui, Nabil Safta*

Unité de Physique Quantique, Faculté des Sciences, Université de Monastir, Avenue de l'Environnement, 5000 Monastir, Tunisia

Email address:
saftanabil@yahoo.fr (N. Safta)

To cite this article
Saber Marzougui, Nabil Safta. A Theoretical Study of the Electronic Properties of $Cd_{1-x}Zn_xS$ quantum Dot Superlattices. *American Journal of Nanoscience and Nanotechnology.* Vol. 2, No. 3, 2014, pp. 45-49. doi: 10.11648/j.nano.20140203.13

Abstract: The present work is aimed to investigate theoretically the electronic properties of superlattices based on $Cd_{1-x}Zn_xS$ quantum dots embedded in an insulating material. This system, considered as a series of flattened cylindrical quantum dots with a finite barrier at the boundary, is studied using the tight binding approximation. The ground miniband width and the longitudinal effective mass have been computed, for the electrons, versus the Zn composition and the inter-quantum dot separation as well. An analysis of the results shows that the Zn compositions x = 0.4 and x = 0.6 are appropriate to give rise a superlattice behavior for conduction electrons in a range of inter –sheet separations studied.

Keywords: Quantum Dots, Superlattices, $Cd_{1-x}Zn_xS$, Tight Binding Approximation, Non Volatile Memories

1. Introduction

The high potentialities of quantum dots (QDs) based on the $Cd_{1-x}Zn_xS$ ternary alloy, have been demonstrated in many device applications [1-3]. In epitaxy, there has also been a development in the growth of $Cd_{1-x}Zn_xS$ QDs [4-7]. Experimentally, some investigations have been dedicated to $Cd_{1-x}Zn_xS$ QDs using different characterization techniques [8-10].

To study the $Cd_{1-x}Zn_xS$ QDs, most approaches have considered that electrons and holes are confined in a spherical QD of radius R and used an infinite potential barrier model [4, 11-14]. For our part, we have, also, adopted, in a first time, the spherical geometry. But to describe the potential energy, we have proposed a potential with a finite barrier at the boundary [15, 16]. The latter potential has the advantage to consider the coupling between QDs. Nevertheless, it presents a big difficulty concerning the determination of the band edges for coupled QDs. In order to around this difficulty, we have suggested the flattened cylindrical geometry with a finite potential barrier at the boundary to describe the QDs [17-21]. Thus, in a first time, we have calculated the energy level structure for a single and double quantum dot [17]. In a second time, we have studied superlattices based on $Cd_{1-x}Zn_xS$ quantum dots embedded in an insulating material using several models. All these studies have been carried out as a function of inter-quantum dot separation for different zinc compositions. More precisely, we have used, in a first work, the Kronig-Penney method to illustrate the confinement potential. Within this model, we have calculated the ground and the first excited minibands as well as the longitudinal effective mass for both electrons and holes [18]. We have proposed, in a second work, the sinusoidal potential to study the ground and the first excited minibands for electrons [19]. In a third work, using the triangular potential model, we have calculated, for electrons, heavy holes and light holes, the Γ_1 − miniband and the longitudinal effective mass as well [20].

The aim of the present work is to investigate the coupling in superlattices made by $Cd_{1-x}Zn_xS$ QDs having a flattened cylindrical geometry with a finite potential barrier at the boundary. Calculations have been made, for the electrons, as a function of Zn composition going from CdS to ZnS using the Tight Binding approximation (TBA). Our interest is focused on the Γ_1 − miniband width and the longitudinal effective mass as well. After an introduction, we report an outline on the theoretical formulation. Discussion of results and conclusions are presented in the following.

2. Theoretical Formulation

Fig. 1- a depicts the geometry used to describe a chain of $Cd_{1-x}Zn_xS$ QDs. The common confined direction is denoted by z. The inter-quantum dot separation is labelled d which corresponds to the period of the structure. Along a common direction of spherical $Cd_{1-x}Zn_xS$ QDs, electrons and holes

see a succession of flattened cylinders of radius R and effective height L. According to that given in Ref [4], the diameter D = 2R varies from 9 nm to 4 nm going from CdS to ZnS. Thus, if we consider L = 1 nm which corresponds to the value reported in Ref [17], one can remark that L is lower than D and consequently the quantum confinement along transversal direction can be disregarded. Therefore, the $Cd_{1-x}Zn_xS$ multi – quantum dot system being studied can be considered as a QDs superlattice along the longitudinal confined direction. Thus, the system to investigate is a $Cd_{1-x}Zn_xS$ QD superlattice where the $Cd_{1-x}Zn_xS$ flattened cylinders QDs behave as wells while the host dielectric lattice forms a barrier of height U_0. For the sake of simplicity, the electron and hole states are assumed to be uncorrelated. The problem to solve is, then, reduced to those of one particle in a one dimensional potential. In this work, we consider the potential depicted in Fig. 1- b. Such a potential can be expressed as:

$$V_{e,h}(z) = \sum_n U_{e,h}(z - nd) \quad (1)$$

with

$$U_{e,h}(z) = \begin{cases} -U_{0e,h}; & -L/2<z<L/2 \\ 0; & L/2<z<d-L/2 \end{cases}$$

The subscripts *e* and *h* refer to electrons and holes respectively and n is the nth period. For this potential, the electron and hole states can be calculated using the effective Hamiltonian:

$$H_{e,h} = \frac{-\hbar^2}{2m^*_{e,h}} \frac{d^2}{dz^2_{e,h}} + V_{e,h}(z_{e,h}) \quad (2)$$

where $\hbar$ is the Plank's constant and m^* is the effective mass of carriers. In deriving the Hamiltonian $H_{e,h}$, we have adopted the effective mass theory (EMT) and the band parabolicity approximation (BPA). The difference of the effective mass between the well and the barrier has been neglected.

We have resolved the Schrodinger equation using the Tight Binding Approximation. Our interest is focused on the longitudinal dispersion relation which shows the k-dependence of minibands along the [001] direction. Our calculation shows that, in the case of the ground miniband (Γ_1 – miniband), this relation is given by:

$$E_{e,h}(k_z) = \left(E_{1e,h} - U_{0e,h}\right) + \frac{2\gamma_{e,h} + 2\beta_{e,h}\cos(k_z d)}{1 + 2r_{e,h}\cos(k_z d)} \quad (3)$$

where E_{1e} corresponds to the ground state energy of electrons associated with an isolated flattened cylindrical quantum dot of $Cd_{1-x}Zn_xS$. E_{1e} is calculated in such a way that the zero energy is taken at the bottom of the QD well [17, 21].

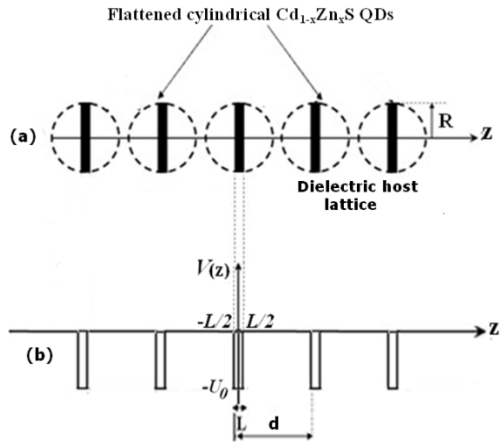

Figure 1. *(a) A schematic diagram of $Cd_{1-x}Zn_xS$ QD superlattices according to the flattened cylindrical geometry – (b) The barrier potential in the framework of the Tight Binding Approximation.*

r_e, β_e and γ_e are respectively, the wave function overlap, the exchange and the correlation integrals. These parameters are, respectively, given by:

$$r_{e,h} = (d-L)\, B_{e,h}^2\, e^{-\rho_{e,h}(d-L)} + \frac{B_{e,h}^2\, e^{-\rho_{e,h} d}}{\rho_{e,h}} + \frac{4A_{e,h}B_{e,h}\, e^{-\rho_{e,h}\left(d-\frac{L}{2}\right)}}{\rho_{e,h}^2 + k_{e,h}^2}\left(\rho_{e,h}\cos\left(\frac{k_{e,h}L}{2}\right) sh\left(\frac{\rho_{e,h}L}{2}\right) + k_{e,h}\sin\left(\frac{k_{e,h}L}{2}\right) ch\left(\frac{\rho_{e,h}L}{2}\right)\right)$$

$$\beta_{e,h} = -\frac{2U_{0e,h}\, A_{e,h}B_{e,h}\, e^{-\rho_{e,h}\left(d-\frac{L}{2}\right)}}{\rho_{e,h}^2 + k_{e,h}^2}\left(\rho_{e,h}\cos\left(\frac{k_{e,h}L}{2}\right) sh\left(\frac{\rho_{e,h}L}{2}\right) + k_{e,h}\sin\left(\frac{k_{e,h}L}{2}\right) ch\left(\frac{\rho_{e,h}L}{2}\right)\right)$$

$$\gamma_{e,h} = -\frac{U_{0e,h}B_{e,h}^2\, e^{\rho_{e,h}(L-2d)}}{\rho_{e,h}}\, sh\left(\frac{\rho_{e,h}L}{2}\right)$$

with

$$A_{e,h} = \left[\frac{L}{2} + \frac{\cos^2\left(\frac{k_{e,h}L}{2}\right)}{\rho_{e,h}} + \frac{\sin(k_{e,h}L)}{2k_{e,h}}\right]^{-\frac{1}{2}}$$

$$B_{e,h} = A_{e,h}\cos\left(\frac{k_{e,h}L}{2}\right)$$

$$k_{e,h} = \sqrt{\frac{2m^*_{e,h}E_{1e,h}}{\hbar^2}}; \quad \rho_{e,h} = \sqrt{\frac{2m^*_{e,h}\left(U_{0e,h} - E_{1e,h}\right)}{\hbar^2}}$$

If we neglect the wave function overlap, the longitudinal dispersion relation becomes:

$$E_{e,h}(k_z) = \left(E_{1e,h} - U_{0e,h}\right) + 2\gamma_{e,h} + 2\beta_{e,h}\cos(k_z d) \quad (4)$$

3. Results and Discussion

We have computed, for electrons, the longitudinal dispersion relation of Γ_1 −miniband, given by Eq. (4), as a function of the ZnS molar fraction, for superlattice periods going from d = 1.5 nm to d= 2.5 nm. Values of parameters used in this computation are summarized in Table 1. All these parameters are taken from Refs [17, 21]. Values of the electron effective mass for $Cd_{1-x}Zn_xS$ with different Zn compositions have been deduced using the Vegard's law. Fig. 2 illustrates the k_z – dependent energy for the CdS and ZnS QD systems in the case of d = 1.5 nm.

Table 1. *Parameters used to calculate the* Γ_{1e} *- miniband for* $Cd_{1-x}Zn_xS$ *QD superlattices.*

x	$\frac{m_e^*}{m_0}$	U_{0e}(eV)	L(nm)	E_{1e}(eV)
0.0	0.16	0.10	1.0	0.090
0.2		0.25	1.0	0.187
0.4		0.45	1.0	0.292
0.6		0.75	1.0	0.384
0.8		1.50	1.0	0.531
1.0	0.28	2.00	1.0	0.560

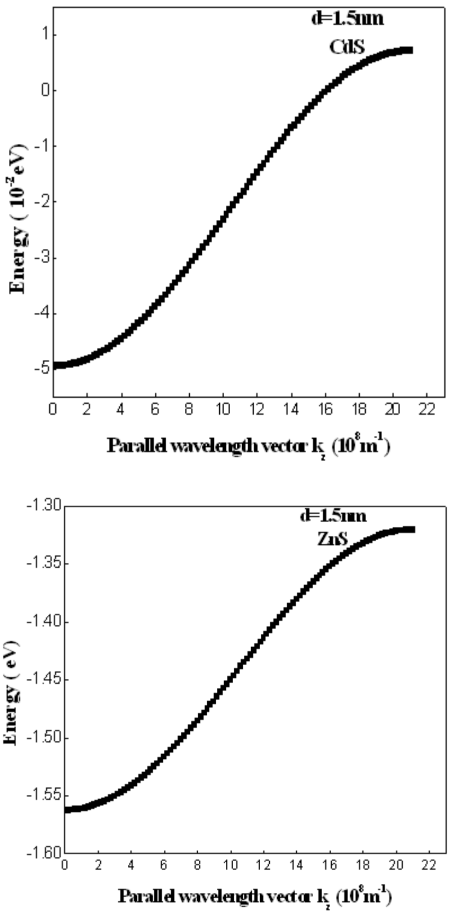

Figure 2. *The* k_z *– dependent energy of the* Γ_1 *- miniband for CdS and ZnS QD systems.*

It is worth to notice that, from the longitudinal dispersion relation curve, one can easily deduce the Γ_1 - miniband width ΔE_{1e}. Thus, we have carried out this parameter for all the compositions and superlattice periods studied. Typical results are depicted in Table 2.

This study led to the following observations: (i) ΔE_{1e} exhibits a decreasing tendency when d increases independently of the Zn composition. As a consequence, the coupling, between nanoparticles decreases as the inter – quantum dot separation increases. This behaviour shows that this coupling is governed by the tunnelling effect for shorter SL periods (ii) for x = 0, ΔE_{1e}, being low, is practically independent of the inter – QD separation. In this case, $Cd_{1-x}Zn_xS$ nanocrystallites are nearly isolated (iii) for x = 0.2, ΔE_{1e} presents a small variation as a function of superlattice period. The coupling between QDs is not high (iv) for large ZnS molar fractions (x= 0.8 – 1.0), the coupling shows a significant decline as the inter – quantum dot separation increases. In this composition range, the QDs can be considered as isolated at high SL periods (v) for intermediate zinc compositions (x = 0.4 – 0.6), the order of magnitude of ΔE_{1e} is important independently of the inter-quantum dot separations. This result reflects the strong degree of coupling between the QDs in this composition range. Since the well width L being the same and the bulk effective mass m_e^* remains practically unchanged for all Zn compositions, these results are, most probably, related to the barrier potential height U_{0e} and the energy E_{1e} values.

Table 2. *The* Γ_1 *- miniband width, as calculated for electrons versus the ZnS molar fraction for different inter-QD separations.*

d (nm)	1.5	1.7	1.9	2.1	2.3	2.5
x						
0.0	0.056	0.054	0.052	0.050	0.048	0.046
0.2	0.211	0.189	0.169	0.151	0.135	0.121
0.4	0.352	0.294	0.242	0.201	0.167	0.139
0.6	0.406	0.302	0.224	0.166	0.123	0.091
0.8	0.344	0.208	0.125	0.076	0.045	0.027
1.0	0.241	0.126	0.065	0.034	0.017	0.009

Let us now discuss the longitudinal electron effective mass m^*_{e,Γ_1} as calculated for the $Cd_{1-x}Zn_xS$ QDs studied. At the vicinity of the minima, Eq. (4) can be rewritten as:

$$E_{e,h}(k_z) = (E_{1e,h} - U_{0e,h}) + 2\gamma_{e,h} + 2\beta_{e,h}\ (1 - \frac{k_z^2 d^2}{2}) \qquad (5)$$

On the other hand, at the vicinity of the minima, we can adopt a parabolic line to the miniband dispersion. Thus, we can write:

$$E_{e,h}(k_z) = (E_{1e,h} - U_{0e,h}) + 2\gamma_{e,h} + 2\beta_{e,h} + \frac{\hbar^2 k_z^2}{2m^*_{e,\Gamma_1}} \qquad (6)$$

From Eqs (5) and (6), we can deduce:

$$m^*_{e,\Gamma_1} = \frac{\hbar^2}{2|\beta_e|d^2} \quad (\beta_e < 0) \tag{7}$$

We have calculated m^*_{e,Γ_1} versus composition x for the different inter – QD separations studied. All these effective masses are expressed in units of the free electron mass m_0. Results are reported in Table 3. Besides, these results were fitted by polynomial laws as a function of x, for the different SL periods studied, and summarized in Table 4.

Table 3. *The longitudinal electron effective mass calculated as a function of the inter-sheet separation for $Cd_{1-x}Zn_xS$ QD superlattices*

d (nm)	1.5	1.7	1.9	2.1	2.3	2.5
x						
0.0	1.194	0.974	0.806	0.692	0.599	0.522
0.2	0.308	0.269	0.250	0.227	0.218	0.207
0.4	0.189	0.176	0.175	0.173	0.171	0.169
0.6	0.164	0.175	0.185	0.226	0.243	0.253
0.8	0.204	0.250	0.317	0.456	0.547	0.768
1.0	0.279	0.405	0.603	0.797	1.573	2.767

Table 4. *The fit of the calculated electron effective (in units of m_0) versus x for different inter-QD separations*

Superlattice period (nm)	Polynomial law
1.5	$1.168-5.507x+8.924x^2- 4.336x^3$
1.7	$0.953-4.351x+6.921x^2-3.134x^3$
1.9	$0.788-3.330x+4.894x^2-1.763x^3$
2.1	$0.681-2.943x+4.545x^2-1.763x^3$
2.3	$0.574-1.474x-0.189x^2+2.637x^3$
2.5	$0.479+0.119x-5.934x^2+8.057x^3$

An analysis of the obtained results leads to the following remarks: (i) for all the inter – quantum dot separations studied, m^*_{e,Γ_1} is shown to decrease with Zn composition up to x = 0.4 or x = 0.6 and it increases, practically, in the same way as x increases from 0.4 or 0.6 to 1.0 (ii) for x = 0.0 and 0.2, m^*_{e,Γ_1} values are ensured by the inter – quantum dot separation rather than the exchange integral (iii) for high zinc compositions, m^*_{e,Γ_1} values are mainly governed by the exchange integral. Moreover, these values are rather high especially for high SL periods (iv) For $Cd_{1-x}Zn_xS$ QDs with intermediate zinc contents, it is of particular interest that the SL period does not significantly affect the longitudinal electron effective mass. In addition, the latter electron band parameter is, in this composition range, practically the same as the one in bulk $Cd_{1-x}Zn_xS$.

4. Conclusion

We investigated the coupling in superlattices made by $Cd_{1-x}Zn_xS$ QDs for compositions ranging from CdS to ZnS. To describe the QDs, we have suggested the flattened cylindrical geometry with a finite potential barrier at the boundary. Using the Tight Binding Approximation, we have calculated, for electrons, the Γ_1 - miniband and the longitudinal electron effective mass. Calculations have been made as a function of Zn composition for different inter – quantum dot separations.

An analysis of the obtained results has evidenced that the Zn compositions x = 0.4 and x = 0.6 are appropriate to give rise a superlattice behavior for conduction electrons in a range of inter –sheet separations studied. As for the longitudinal electron effective mass, it is found to be the lower for x = 0.4 and x = 0.6.

In the applied physics, this study could be useful for designing a new category of nanocrystal devices based on well controlled $Cd_{1-x}Zn_xS$ QDs especially the non – volatile memories.

References

[1] A. J. Peter and C. W. Lee.(2012), Electronic and optical properties of CdS/CdZnS nanocrystals, Chinese Phys. B 21: 087302.

[2] L. Zhou, Y. Xing and Z. P. Wang(2012), Hydrogenic impurity bound polaron in a quantum dot quantum well structure, Eur. Phys. J. B. 85: 212.

[3] F. Scotognella, G. Lanzani, L. Manna, F. Tassone and M. Zavelani-Rossi. (2012), Study of higher-energy core states in CdSe/CdS octapod nanocrystals by ultrafast spectroscopy, Eur. Phys. J. B. 85: 128.

[4] B. Bhattacharjee, S. K. Mandal, K. Chakrabarti, D. Ganguli and S. Chaudhui. (2002), Optical properties of $Cd_{1-x}Zn_xS$ nanocrystallites in sol–gel silica matrix, J. Phys. D: Appl. Phys. 35: 2636-2642.

[5] L. Cao, S. Huang and S. E. (2004), ZnS/CdS/ZnS quantum dot quantum well produced in inverted micelles, J. colloid Interface Sci. 273: 478-482.

[6] H. Kumano, A. Ueta and I. Suemune. (2002), Modified spontaneous emission properties of CdS quantum dots embedded in novel three-dimensional microcavities, Physica E 13: 441-445

[7] Y. C. Zhang, W. W. Chen and X. Y. Hu. (2007), In air synthesis of hexagonal $Cd_{1-x}Zn_xS$ nanoparticles from single-source molecular precursors, Mater. Lett. 61: 4847-4850

[8] C. S. Pathak, D. D. Mishra, V. Agarawala, M. K. Mandal. (2012), Mechanochemical synthesis, characterization and optical properties of zinc sulphide nanoparticles, Indian J. Phys 86: 777-781.

[9] S. Roy, A. Gogoi and G. A. Ahmed. (2010), Size dependent optical characterization of semiconductor particle: CdS embedded in polymer matrix, Indian J. Phys. 84: 1405-1411

[10] A. U. Ubale and A. N. Bargal. (2010), Characterization of nanostructured photosensitive cadmium sulphide thin films grown by SILAR deposition technique, Indian J. Phys. 84: 1497-1507

[11] K.K Nanda, S.N. Sarangi, S. Mohanty, S.N. Sahu. (1998), Optical properties of CdS nanocrystalline films prepared by a precipitation technique, Thin Solid Films 322: 21-27.

[12] H. Yükselici, P. D. Persans and T. M. Hayes.(1995), Optical studies of the growth of Cd1-*x*Zn*x*S nanocrystals in borosilicate glass, Phys. Rev. B. 52: 11763.

[13] Q. Pang, B.C. Guo, C.L. Yang, S. H. Yang, M.L. Gong, W.K. Ge and J. N. Wang. (2004), Cd_1–xMnxS quantum dots: new synthesis and characterization, Journal of Crystal Growth, 269: 213-217.

[14] M.C. Klein, F. hache, D. Ricard and C. Flytzanis. (1990), Size dependence of electron-phonon coupling in semiconductor nanospheres: The case of CdSe, Phys Rev. B. 42: 11123.

[15] N. Safta, A. Sakly, H. Mejri and Y. Bouazra. (2006), Electronic and optical properties of $Cd_{1-x}Zn_xS$ nanocrystals, Eur. Phys. J. B 51: 75-78

[16] A. Sakly, N. Safta, A. Mejri, H. Mejri, A. Ben Lamine. (2010), The Excited Electronic States Calculated for Cd1-*x*Zn*x*S Quantum Dots Grown by the Sol-Gel Technique, J. Nanomater, ID746520.

[17] N. Safta, A. Sakly, H. Mejri and M. A. Zaïdi. (2006), Electronic properties of multi-quantum dot structures in $Cd_{1-x}Zn_xS$ alloy semiconductors, Eur. Phys. J. B 53: 35 – 38

[18] A. Sakly, N. Safta, H. Mejri, A. Ben Lamine. (2009), The electronic band parameters calculated by the Kronig–Penney method for Cd_1–xZnxS quantum dot superlattices, J. Alloys Compd. 476: 648–652.

[19] A. Sakly, N. Safta, H. Mejri, A. Ben Lamine. (2011), The electronic states calculated using the sinusoidal potential for Cd_1–xZnxS quantum dot superlattices, J. Alloys Compd.509: 2493–2495

[20] S. Marzougui, N. Safta. (2014),The electronic band parameters calculated by the Triangular potential model for $Cd_{1-x}Zn_xS$ quantum dot superlattices, IOSR-JAP 5 (5) : 36-42

[21] S. Marzougui. (2011), *A study of the excited states in the flattened cylindrical quantum dots of* $Cd_{1-x}Zn_xS$, Master, University of Monastir.